

# Utilization of genomic signatures to identify high-efficacy candidate drugs for chemorefractory endometrial cancers

Budiman Kharma<sup>1</sup>, Tsukasa Baba<sup>1</sup>, Masaki Mandai<sup>1</sup>, Noriomi Matsumura<sup>1</sup>, Susan K. Murphy<sup>2</sup>, Hyun Sook Kang<sup>1</sup>, Koji Yamanoi<sup>1</sup>, Junzo Hamanishi<sup>1</sup>, Ken Yamaguchi<sup>1</sup>, Yumiko Yoshioka<sup>1</sup> and Ikuo Konishi<sup>1</sup>

<sup>1</sup> Department of Gynecology and Obstetrics, Kyoto University Graduate School of Medicine, Kyoto, Japan

<sup>2</sup> Division of Gynecologic Oncology, Department of Obstetrics and Gynecology, Duke University Medical Center, Durham, NC

Endometrial cancer, one of the most common gynecologic malignancies, is increasing in Japan, nearly doubling over the last decade. High-grade disease patients are often resistant to conventional chemotherapy with platinum agents; therefore, discovery of efficacious new drugs in this setting is required to benefit chemorefractory cases. The 50% growth-inhibitory (GI50) concentration of 27 clinically relevant drugs was measured in the NCI60 panel of cell lines. Gene expression data were analyzed using Bayesian binary regression, to first generate a response signature for each drug and then to calculate individual susceptibility scores using *in vivo* endometrial cancer data (GSE2109; <http://www.ncbi.nlm.nih.gov/geo>) and *in vitro* data (GSE25458), as well as to identify candidate drugs for chemorefractory cases. Using these candidates, cell proliferation, apoptosis and caspase assays were performed *in vitro*. The tumor growth-inhibitory effect of the candidate was also assessed *in vivo* using nude mice. Through microarray analysis, fludarabine and temsirolimus showed higher susceptibility scores in high-grade cases compared to cisplatin, doxorubicin and paclitaxel. Fludarabine significantly inhibited cell proliferation and increased apoptosis in the cisplatin-resistant endometrial cancer cell line, HEC1A, relative to HEC50B ( $p < 0.001$ ). Fludarabine treatment also enhanced caspase-3/7 activity in HEC1A relative to HEC50B cells ( $p < 0.001$ ), and inhibited the growth of HEC1A xenograft tumors relative to cisplatin ( $p < 0.05$ ). These results support that identification and use of genomic signatures can lead to identification of new therapeutic candidates that may prove beneficial to chemoresistant cases. Fludarabine may be useful in targeting high-grade, chemorefractory endometrial cancer.

Endometrial cancer is the leading cause of gynecologic malignancy with 43,470 estimated cases diagnosed per year and 7,950 annual death in the United States, respectively, consisting of 6% of new cancer cases and 3% of all cancer deaths, and disease incidence has been steadily increasing.<sup>1,2</sup> The majority of endometrial cancers, more than 80%, are diagnosed at an early stage with the disease located within the uterus. When diagnosed at an early stage, primary surgery is frequently curative enough to be associated with a favorable prognosis. In contrast, extrauterine spread of cancer cells profoundly impacts patient prognosis as previous studies revealed high hazard ratios for Stage III and Stage IV compared to Stage I disease.<sup>2</sup> Clear cell and papillary serous

carcinomas of the uterus are associated with aggressive behaviors, even at an early stage, with 5-year survival between 60 and 66%.<sup>3</sup> Besides staging and histology, several pathological factors, such as tumor grade, depth of invasion and lymph vascular invasion, are well known to determine the prognosis of each patient with an aggressively metastatic phenotype. Recently, adjuvant chemotherapy has been introduced after primary surgery as part of the first-line management for preventing recurrence of such high-risk disease.<sup>4</sup> First-line chemotherapy typically consists of a combination regimen followed by treatment with a single agent on disease progression. Throughout the phase II and III studies of the Gynecologic Oncology Group (GOG), platinum combined with doxorubicin and/or taxane has played an important role in the treatment of high-risk disease, but was also associated with infrequent complete response with recurrence in nearly half of these patients. Furthermore, there is no active second-line agent after failure of primary chemotherapies, as the response rate to paclitaxel was at most 25% for recurrent patients previously treated with doxorubicin and cisplatin.<sup>5</sup> With the objective of improving the prognosis of those with high-risk disease, it is essential to identify candidate cytotoxic agents that are effective against patients with resistance to conventional chemotherapies (chemorefractory tumors) or supportive agents that increase sensitivity to primary chemotherapies.

**Key words:** chemoresistant, fludarabine, chemodynamics, endometrial cancer

Additional Supporting Information may be found in the online version of this article.

**Conflict of interest:** Nothing to report.

**DOI:** 10.1002/ijc.28220

**History:** Received 1 Mar 2013; Accepted 3 Apr 2013; Online 18 Apr 2013

**Correspondence to:** Tsukasa Baba, 54 Shogoin Kawahara-cho, Sakyo-ku, Kyoto 606-8507, Japan, Tel.: 81-75-751-3269, Fax: 81-75-761-3967, E-mail: babatsu@kuhp.kyoto-u.ac.jp

**What's new?**

Patients with advanced endometrial cancer need something beyond conventional therapies. Genome wide microarray analysis of these difficult-to-treat cancers has shown that they have distinctive genetic signatures. In this paper, the authors profiled drug-resistant endometrial cancer cell lines to identify potentially effective chemical therapies. From their analysis, they determined that five of seven cancer cell lines were likely susceptible to the chemotherapy agent fludarabine. They then demonstrated fludarabine's toxicity *in vitro* and *in vivo*, suggesting the drug may have promise for treating the cancer.

Identification of effective second-line agents for chemorefractory cancers has been a long-sought goal, and over the past few years various new cytotoxic agents have been synthesized for the treatment of malignancies. Clinical trials for endometrial cancer have also historically been conducted using drugs identified as effective for other solid malignancies, especially ovarian cancer. However, these trial-and-error approaches to drug mining are inefficient for this heterogeneous entity "endometrial cancer," and have mostly failed. To elevate the efficacy of second-line chemotherapy, individualized therapy will be necessary based on biological features of the patient and tumor, such as molecular mechanisms and clinical phenotypes.

Recent development of genome-wide analysis with microarray has revealed that chemorefractory cancers possess characteristic gene expression profiles, so called chemoresistant signatures.<sup>6,7</sup> A computational analysis using Bayesian binary regression methods enabled to project a phenotype signature extracted from one microarray onto another microarray to predict the phenotype probability of each sample in projected microarray. In our study, we utilized this bioinformatics approach to demarcate that fludarabine had potential efficacy in chemorefractory endometrial cancers. Furthermore, we performed several *in vitro* and *in vivo* approaches using endometrial cancer cell lines to demonstrate that fludarabine may be a potential alternative treatment for chemorefractory endometrial cancers.

**Material and Methods****Patients**

Clinicopathological information of 262 patients treated for endometrial cancer during 2004–2011 in Kyoto University Hospital was obtained with written consent from each patient and used under protocols approved by the Kyoto University Institutional Review Board. The prognostic risk of each case was determined as low, intermediate or high, as previously described.<sup>8</sup>

**Cell lines and culture**

Human endometrial cancer cell lines, AN3CA, HEC1A, HEC1B, KLE, RL95-2, TEN (ATCC, Rockville, MD), ACC230, ACC564 (DSMZ, Brunswick, Germany), HHUA, Ishikawa, JHUEM-1, JHUEM-2, JHUEM-3, JHUEM-7, JHUEM-14, Sawano (RIKKEN BRC, Tsukuba, Japan), HEC50B, HEC108, HEC265 and SNG-M (JCRB, Osaka, Japan), were maintained in RPMI1640 (Nikken, Kyoto, Japan) or DMEM/Ham's F12 (Invitrogen, Carlsbad, CA) supplemented with 10% heat-inactivated fetal bovine serum (v/v;

Biowest, France) and penicillin–streptomycin (100 IU/ml penicillin and 100 µg/ml streptomycin; Nacalai Tesque, Kyoto, Japan). All cells were seeded into Cellstars<sup>®</sup> tissue culture plates (Greiner, Frickenhausen, Germany) and used for experiments after 18-hr incubation.

**Chemicals**

Following the manufacturer's instructions, a 5 mM stock solution of fludarabine (Alexis Biochemicals, San Diego, CA) was prepared in cold sterile water and stored at  $-20^{\circ}\text{C}$ . Fresh thawed dilutions were used for each experiment. A 3.33 mM stock solution of cisplatin (Sigma Aldrich, St Louis, MO) was also prepared in sterile water following the manufacturer's instructions.

**Bioinformatics analyses**

Total RNA was extracted from cell lines using the RNeasy<sup>®</sup> Mini Kit (QIAGEN, Valencia, CA), and gene expression microarray data (Affymetrix U133 Plus 2.0) were generated in triplicate and robust multi-array average-normalized as described previously.<sup>9</sup> Expression microarray data of endometrial cancers (GSE2109) were also obtained from the Gene Expression Omnibus web site (<http://www.ncbi.nlm.nih.gov/geo>). Gene expression data for NCI60 cell lines were obtained from the National Cancer Institute along with 50% growth-inhibitory (GI50) values for 27 commercially available chemotherapeutic agents (<http://www.dtp.nci.nih.gov/webdata.html>). GI50 value data for 27 drugs from the NCI60 cell line data were normalized with median centering using Cluster 3.0 (<http://rana.lbl.fgov/EisenSoftware.htm>) and converted into a visual representation using JavaTreeView (<http://jtreeview.sourceforge.net/>). Heat maps were generated using Matlab (Mathworks, Natick, MA) or R with Bioconductor (<http://www.r-project.org/>) as described previously.<sup>9–11</sup> Genomic signatures of drug susceptibility were generated using Bayesian binary regression<sup>10</sup> from gene expression data of ten sensitive and ten resistant cell lines from the NCI60 drugs screening panel. Probabilities of chemosensitivity in response to NCI60 drugs were scored for each sample in dataset GSE 25458 as previously described.<sup>9</sup>

**Cell proliferation assay**

AN3CA, HEC1A and HEC50B cells were seeded into 96-well tissue culture plates at  $2 \times 10^3$  cells per well. The cell culture medium was replaced with fresh medium containing 0, 10, 25, 50, 100, 250 or 500µM fludarabine and incubated for 24

hr. The number of viable cells in each well was examined using the WST-1 assay kit (Premix WST-1<sup>®</sup>, Takara, Otsu, Japan) following the manufacturer's instructions.

#### Apoptosis detection

AN3CA, HEC1A and HEC50B cells were treated with medium containing 0, 25, 50 or 100  $\mu$ M fludarabine for 24 hr. Cells were harvested by trypsinization for apoptosis detection by flow cytometry. After washing with phosphate-buffered saline, cells were resuspended in 200  $\mu$ l of 1 $\times$  annexin-V binding buffer (BD Pharmingen). Next, 5  $\mu$ l of 7-aminocoumarinyl actinomycin D (7-AAD) (BD Pharmingen) and 5  $\mu$ l of annexin-V were added to the tubes and incubated for 10 min at 4°C in the dark. Cells were washed with 500  $\mu$ l of 1 $\times$  annexin-V binding buffer and then resuspended in 200  $\mu$ l of 1 $\times$  annexin-V binding buffer followed by filtration through a 70- $\mu$ m nylon filter (Becton Dickinson Labware, Franklin Lakes, NJ). The samples were placed on ice and analyzed by FACSCalibur (Becton Dickinson). The data were analyzed using FlowJo v.7.6.3 (Tree Star, Ashland, OR).

Caspase-3/7 activity was measured using the Caspase-Glo<sup>®</sup> 3/7 Assay System (Promega, Madison, WI) following the manufacturer's instructions. After 2-hr incubation with the Caspase-Glo 3/7 Reagent, luminescence was measured using a Glo-Max<sup>®</sup> Luminometer (Promega) as directed by the manufacturer.

#### Western blot

AN3CA, HEC1A and HEC50B cells were treated with medium containing 0, 25, 50 or 100  $\mu$ M fludarabine for 24 hr. Cells were lysed in radioimmunoprecipitation assay (RIPA) buffer (Thermo Fisher Scientific, Waltham, MA) with a protease inhibitor cocktail (EMD, Madison, WI) and a phosphatase inhibitor cocktail (Nacalai Tesque). Protein was quantified using the DC Protein Assay Kit (Bio-Rad, Hercules, CA). Twenty micrograms of sodium dodecyl sulfate (SDS)-treated protein was loaded onto a 10–20% Tris-Tricine Mini Protean<sup>®</sup> gel (Bio-Rad). Gels were electroblotted onto polyvinylidene fluoride membranes (Bio-Rad). Nonspecific binding of the antibody was blocked by 1-hr incubation at room temperature in Blocking One-P (Nacalai Tesque). The membranes were incubated overnight at 4°C with caspase-3 antibody (1:1,000, caspase-3 Rabbit mAb, Cell Signaling Technology, Danvers, MA) or cleaved caspase-3 (Asp175) antibody (1:1,000, cleaved caspase-3 rabbit polyclonal Ab, Cell Signaling Technology). After washing in Tris-buffered saline (TBS)-T, the blots were incubated with the appropriate peroxidase-coupled secondary antibody (1:6,000; anti-rabbit HRP, GE Healthcare Life Sciences, Uppsala, Sweden).  $\beta$ -Actin was used as an endogenous loading control and detected using an anti-human  $\beta$ -actin antibody (1:8,000; Rabbit mAb, Abcam, Cambridge, MA). Specific proteins were detected using ECL Plus Western Blotting Reagent (GE Healthcare Life Sciences). The bands were visualized using

Molecular Imager<sup>®</sup> Gel Doc<sup>™</sup> XR+ and ChemiDoc<sup>™</sup> XRS+ Systems with Image Lab 2.0 software (Bio-Rad).

#### Real-time qPCR

Total RNA was extracted from cell lines using the RNeasy<sup>®</sup> Mini Kit (QIAGEN). To monitor gene expression, quantitative reverse transcriptase (RT)-PCR amplification of human caspase-3 $\alpha$ , caspase-3 $\beta$  and *GAPDH* mRNAs was done by Light Cycler 480-II (Roche, Basel, Switzerland) using a Dual Color Hydrolysis Universal Probe System (Roche). The following primers that were obtained from the Universal Probe Library Assay Design Center (Roche) were used for analysis: caspase-3 $\alpha$ , 5'-CTG GTT TTC GGT GGG TGT-3' (forward), 5'-CCA CTG AGT TTT CAG TGT TCT CC-3' (reverse); caspase-3 $\beta$ , 5'-TGG AAT TGA TGC GTG ATG TT-3' (forward), 5'-TGG CTC AGA AGC ACA CAA AC-3' (reverse); *GAPDH*, 5'-AGC CAC ATC GCT CAG ACA C-3' (forward), 5'-GCC CAA TAC GAC CAA ATC C-3' (reverse). Cycling parameters were 95°C for 10 sec followed by 40 cycles of 95°C for 5 sec and 60°C for 30 sec, followed by a dissociation cycle of 95°C for 15 sec, 60°C for 20 sec and 95°C for 15 sec. The expression of human caspase-3 $\alpha$  and caspase-3 $\beta$  mRNAs was estimated by dividing the caspase-3 $\alpha$  and caspase-3 $\beta$  threshold cycle (CT) values by the *GAPDH* CT values.

#### In vivo experiment

Female CD-1 Foxn/Nu mice were purchased from Oriental Bioservice (Kyoto, Japan). Animal care and experimental procedures under specific pathogen-free conditions were performed in accordance with the guidelines of the Institute of Laboratory Animals Graduate School of Medicine, Kyoto University. Subcutaneous xenografts were established in the flanks by inoculating  $5 \times 10^6$  cells of the AN3CA, HEC1A or HEC50B cell lines. Three days after inoculation, each mouse was treated twice a day for 5 days with intraperitoneal administration of 125 mg/kg fludarabine, 1 mg/kg cisplatin or 50  $\mu$ l sterile distilled water as a control treatment ( $n = 4$  in each arm). Therapeutic effects were monitored by measuring tumor growth for 30 days after inoculation. The differences in tumor growth were analyzed statistically.

#### Statistical analysis

Group comparisons were done using Mann-Whitney *U*-tests. Prognostic analysis was done using log-rank test and Fisher's exact test. Statistical analyses were done using GraphPad Prism 5.5 software. Probability values below 0.05 were considered significant.

## Results

### Clinical significance of current chemotherapy in the treatment of endometrial cancer

Clinical features of the 262 patients studied here are listed in Table 1. Forty-three patients exhibited progression or recurrence of the disease (progressive disease, PD).

Table 1. Patient characteristics. [Color table can be viewed in the online issue, which is available at wileyonlinelibrary.com.]

		<i>n</i>	Recurrence/PD	<i>p</i>	Rate of 5 yr OS	<i>p</i>
Age	≤50	57	3		93.5	
	>50	205	40	0.0083	85.4	0.174
stage	I	174	10		98.5	
	II	19	2	0.3348	100	0.6355
	III	46	13	<0.0001	68.6	<0.0001
	IV	23	18	<0.0001	28.6	<0.0001
Myometrial invasion	≤1/2	145	6		97.0	
	>1/2	109	29	<0.0001	81.1	0.0004
LVSI	-	166	8		96.2	
	+	81	26	<0.0001	77.2	<0.0001
grade	Low	160	7		97.7	
	high	102	36	<0.0001	70.2	<0.0001
risk	Low	86	0		100	
	Intermediate	82	3	0.1141	98.4	0.3293
	high	94	40	<0.0001	64.9	<0.0001

Known risk factors are listed for the patients in our study. Recurrence/PD: the number of patients who showed recurrence or progressive disease during chemotherapy; LVSI means lymphovascular space invasion.

Clinicopathological analysis revealed that each known prognostic factor including advanced stage, outer-half myometrial invasion, lymphovascular space invasion and histological grade showed significant differences both in terms of the rate of PD and in the overall survival (OS) of patients. Based on the prognostic risk classification, 86 patients were categorized as “low-risk” without any PD. Three of 82 “intermediate-risk” patients recurred, but there was no significant difference in OS compared to “low-risk” patients, whereas “high-risk” patients exhibited higher PD and poor OS ( $p < 0.0001$ , Supporting Information Fig. 1). PD was significantly lower among patients who received chemotherapies with cisplatin + doxorubicin and paclitaxel + carboplatin in the “intermediate-risk” group ( $p < 0.05$ , Table 2), whereas not in the “high-risk” group ( $p = 0.72$ ).

#### Drug sensitivity prediction from the NCI60 data

As a first step toward identifying compounds that exhibit efficacy toward chemoresistant endometrial cancer cells, we queried the NCI-60 database for the 50% growth-inhibitory

doses (GI50) of conventional chemotherapeutic agents including cisplatin, paclitaxel and doxorubicin. GI50 values were normalized (see Material and Methods section) and visualized using a heatmap. Based on this representation, normalized GI50 values  $> 0.04$  were colored in red or orange and 0.04 was thus determined as a threshold for sensitivity (Fig. 1a). By this criterion, 24 of 62 cell lines (39%) were resistant to cisplatin, doxorubicin and paclitaxel, and this rate, 39%, was very close to the rate of PD (44%) among the “high-risk” patients in our clinical data.

Second, the GI50 values were obtained from the NCI-60 database for another 24 commonly used chemotherapeutic agents for the 24 chemoresistant cell lines. An unsupervised hierarchical clustering analysis using the normalized GI50 values for the chemoresistant cells revealed that these 24 drugs were divided into two clusters: cluster 1 contains the anticancer drugs, whereas cluster 2 contains molecular targeting drugs (Fig. 1b). Some of the drugs exhibited efficacy against several cell lines, but fludarabine appeared to effectively target ten of these 24 chemoresistant cells.

**Table 2.** Patient chemoresponsiveness profiles. [Color table can be viewed in the online issue, which is available at [wileyonlinelibrary.com](http://wileyonlinelibrary.com).]

	Chemo	n	Recurrence/PD	p
Low	-	75	0	
	+	11	0	-
Intermediate	-	25	3	
	+	57	0	0.0260
High	-	8	4	
	+	86	36	0.7193

Effectiveness of chemotherapy was evaluated in each risk group using Fisher's exact test.

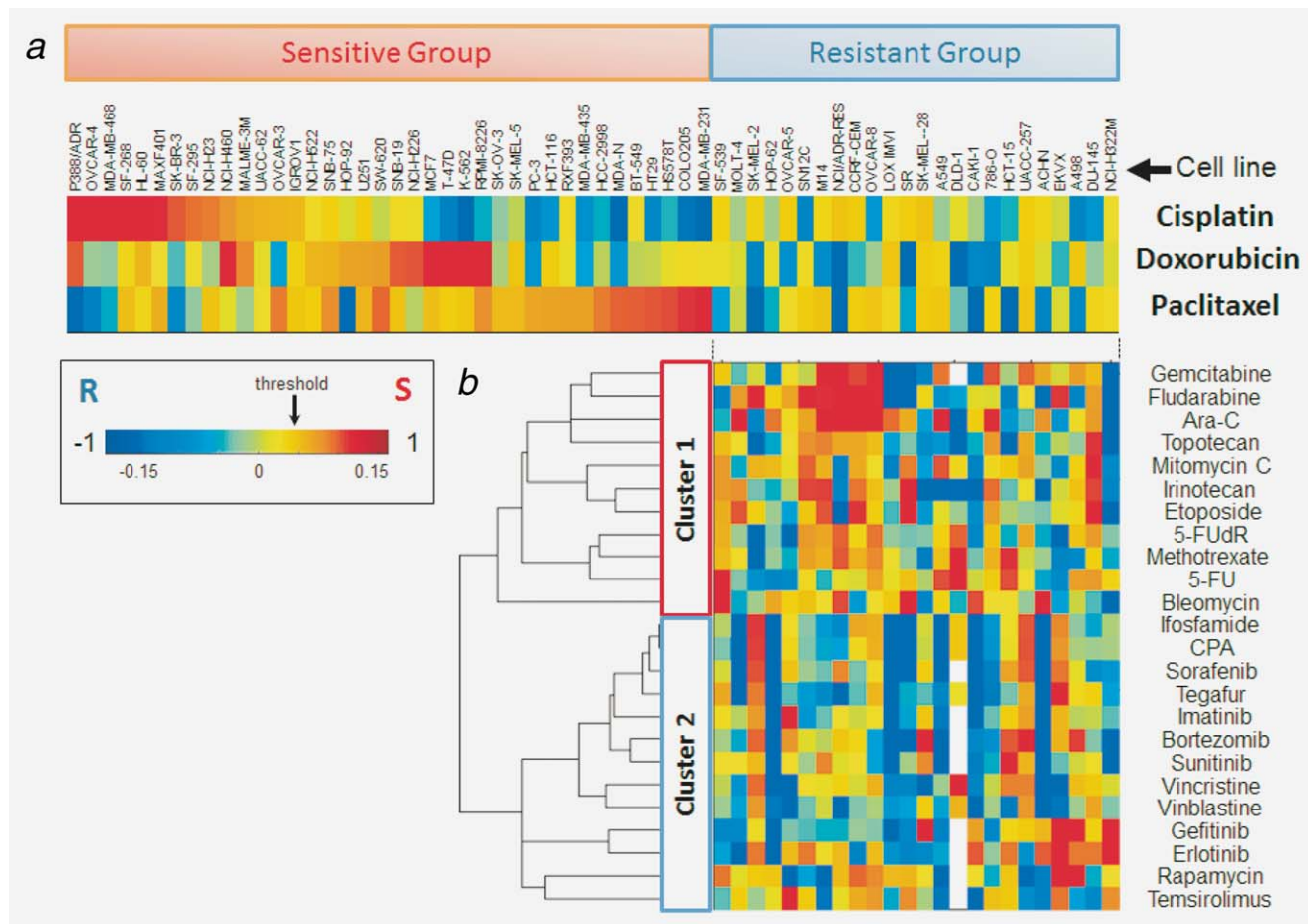


**Figure 1.** The 50% growth-inhibitory doses (GI50) of anticancer drugs in the NCI60 dataset in predicting chemoresponsiveness. (a) NCI60 cell lines were aligned according to their normalized GI50 values for cisplatin, doxorubicin and paclitaxel, shown in the top panel. Most (84.63%) of the normalized GI50 values ranged between 0.15 (red) and -0.15 (blue). Dark red and dark blue at the extreme ends of the color bar represent values >0.15 and <-0.15, respectively. [S: sensitive; R: resistant; threshold indicates the value (0.04) above which cells were considered as chemosensitive] (b) For the 24 chemoresistant cell lines in panel a, GI50 values were obtained for an additional 24 commonly used chemotherapeutic agents. Unsupervised hierarchical clustering produced two clusters: cluster 1 contains anticancer drugs; cluster 2 contains molecular targeting drugs. [Color figure can be viewed in the online issue, which is available at [wileyonlinelibrary.com](http://wileyonlinelibrary.com).]

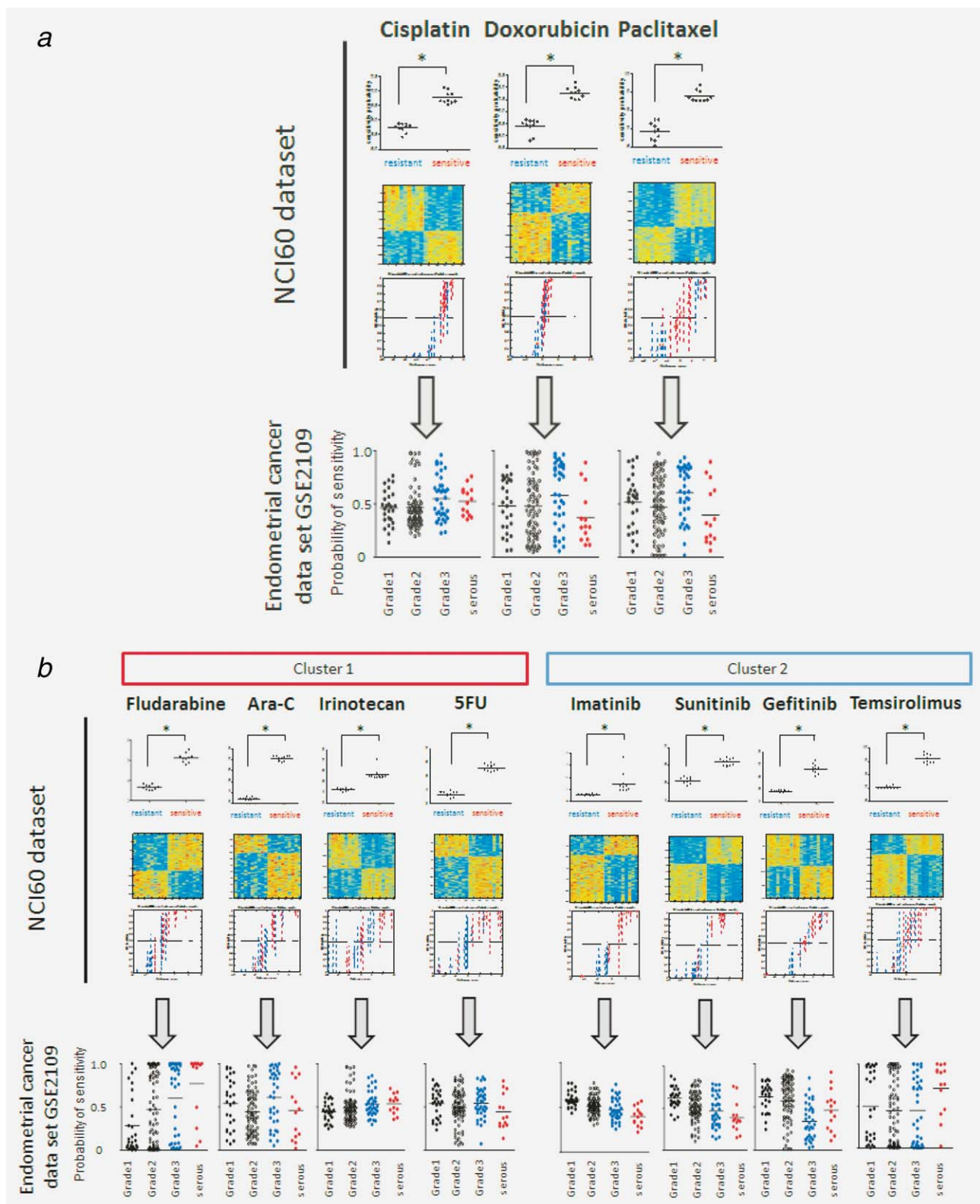


**Figure 2.** Predicted susceptibility of chemo agents in endometrial cancers *in vivo*. (a) Genomic signatures of susceptibility were generated using Bayesian binary regression from the NCI60 gene expression data and applied to microarray data from endometrial cancers in GSE2109 for predicting the probability of sensitivity to cisplatin, doxorubicin and paclitaxel. (b) Drug susceptibility signatures were also developed for fludarabine, Ara-C and irinotecan as representative anticancer drugs from cluster 1, and for tensirolimus, gefitinib and sunitinib as representative molecular targeting drugs from cluster 2. The probability of sensitivity ( $y$ -axis on a scale of 0–1, with 0 indicating high probability of resistance and 1 indicating high probability of sensitivity) to the three conventional chemotherapeutic agents was not superior in Grade 3 endometrioid adenocarcinoma and serous papillary adenocarcinoma to those in low-grade endometrioid adenocarcinoma. On the other hand, the probability of sensitivity to fludarabine was significantly higher in Grade 3 and serous and for tensirolimus was significantly higher in serous ( $p < 0.001$  and  $p < 0.05$ , respectively). (c) Gene expression microarray analysis was performed in 20 endometrial cancer cell lines, and drug-susceptibility signatures for the conventional chemotherapeutic agents were applied to predict the probability of sensitivity of each cell line. Numbers in each box indicate the probability score with colors indicating probability of response. [Color figure can be viewed in the online issue, which is available at [wileyonlinelibrary.com](http://wileyonlinelibrary.com).]

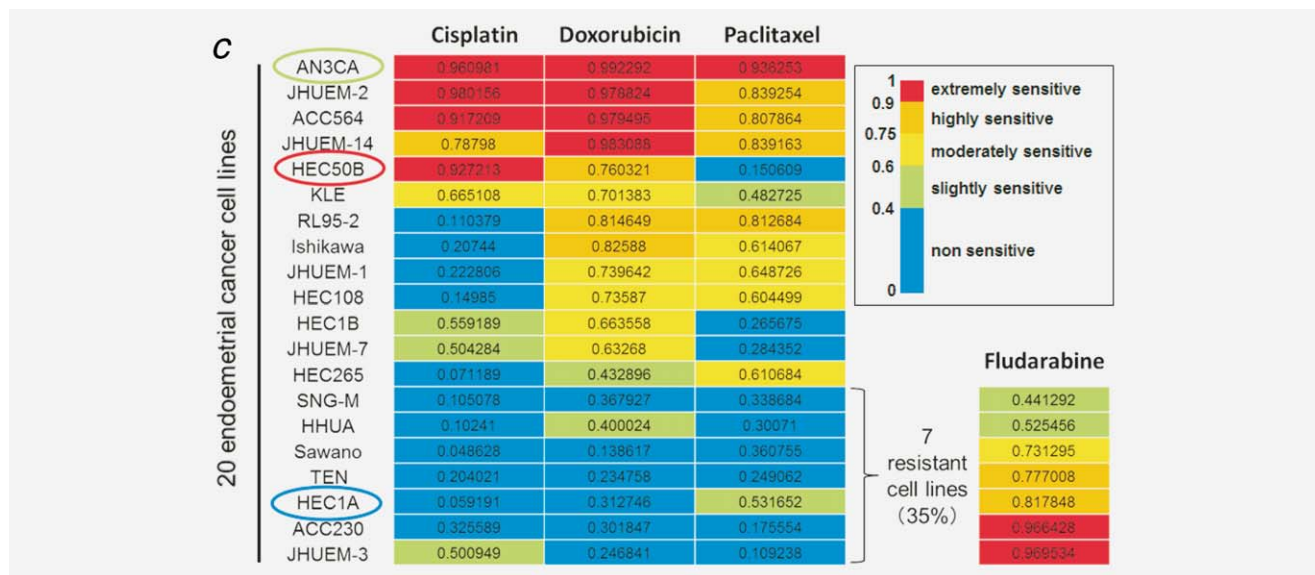


Figure 2. (Continued)

### Predicted susceptibility of chemotherapeutic agents in endometrial cancers

The NCI60 drug screening panel also contains genetic information. By selecting ten sensitive and ten resistant cell lines, a genomic signature of drug susceptibility for each chemotherapeutic agent was derived using Bayesian binary regression<sup>10</sup> from the gene expression data. Such genomic signatures can be applied to an independent gene expression dataset to predict drug susceptibility for each sample in the dataset as previously described.<sup>12</sup> Drug-susceptibility signatures developed from the NCI60 dataset were applied to the microarray data of endometrial cancers in GSE2109 for predicting the probabilities of sensitivity to cisplatin, doxorubicin and paclitaxel. Meanwhile, drug-susceptibility signatures were also developed for fludarabine, Ara-C, irinotecan and 5-FU, as representative cluster 1 anticancer drugs, and for imatinib, gefitinib, sunitinib and temsirolimus, as representative molecular targeting drugs from cluster 2; these drugs were chosen as representative drugs for each subcluster based on chemosignatures for the NCI60 cell lines. The sensitivity probabilities of the three conventional chemotherapeutic agents in Grade 3 endometrioid adenocarcinoma and serous papillary adenocarcinoma were not superior to those in low-grade endometrioid adenocarcinoma (Fig. 2a). On the other hand, the probability of sensitivity to fludarabine was significantly higher in Grade 3 and serous, and the probability of sensitivity to temsirolimus was significantly higher in serous (Fig. 2b;  $p < 0.001$  and  $p < 0.05$ , respectively).

Gene expression microarray analysis was performed in 20 endometrial cancer cell lines, and the drug-susceptibility signatures of conventional chemo agents were applied to predict the sensitivity of each cell line. There was a statistically significant correlation between cisplatin GI50 values of 37

ovarian cancer cell lines<sup>10</sup> and cisplatin sensitivity probability scores derived from the gene expression microarray data (GSE25428,  $r = 0.3776$ ,  $p = 0.02$ , data not shown).

Seven cell lines exhibited low probabilities of sensitivity to cisplatin, doxorubicin and paclitaxel, whereas another 13 cell lines exhibited higher probabilities of sensitivity. Intriguingly, five out of these seven cells showed relatively high probabilities of sensitivity to fludarabine (Fig. 2c), and three had favorable probability scores to temsirolimus (Supporting Information Table 2). Further, we investigated HEC1A as a representative chemorefractory cell line with AN3CA (sensitive to all conventional chemo agents) and HEC50B (partly sensitive to conventional chemo agents) as counterpart controls for further experiments. Fludarabine was selected for further experiments as the most potent alternative agent for chemorefractory cases.

### Cytotoxic activities of fludarabine in vitro

The cytotoxic effect of fludarabine was examined using proliferation assays. AN3CA, HEC1A and HEC50B were exposed to fludarabine (from 0 to 500  $\mu\text{M}$ ) for 24 hr. There were dose-dependent growth-inhibitory responses in the AN3CA and HEC1A cells ( $p < 0.01$ ), and more than 90% growth abrogation was observed in HEC1A cells at 500  $\mu\text{M}$  ( $p < 0.001$ ). There was no significant difference in proliferation after fludarabine treatment for the HEC50B cells at any dose (Fig. 3a).

To investigate the growth-inhibitory mechanism of fludarabine in endometrial cancer cells, annexin-V/7-AAD apoptosis assays were performed using flow cytometry. After 24-hr exposure to fludarabine, apoptosis in AN3CA and HEC1A cells was increased in a dose-dependent manner, with 20 and 25% of the cells undergoing apoptosis after treatment with

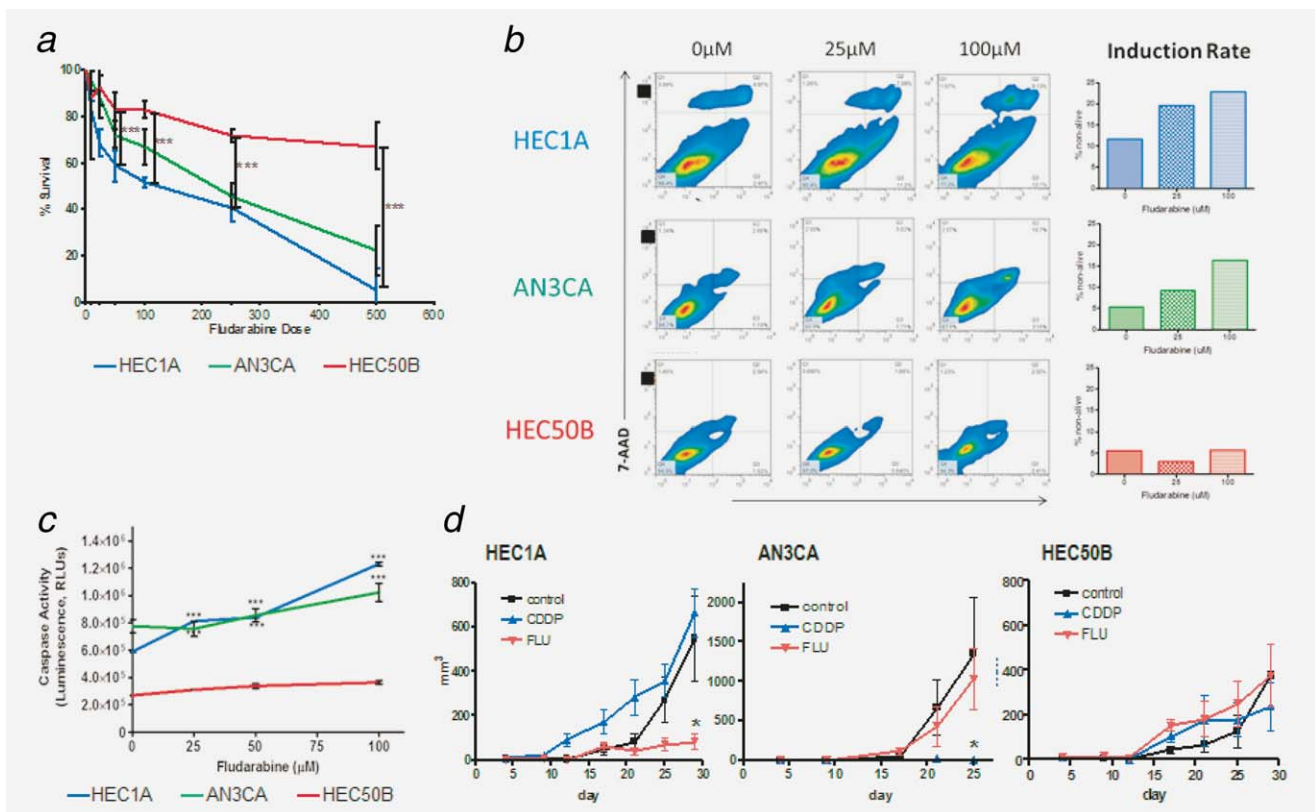


**Figure 3.** Cytotoxic activities of fludarabine. (a) The cytotoxicity of fludarabine was measured using WST-1 cell proliferation assays. There were growth-inhibitory responses in AN3CA (green) and HEC1A (blue) in a dose-dependent manner ( $p < 0.01$ ), whereas this response was not significant in HEC50B (red). (b) Apoptosis induction after fludarabine treatment in HEC1A, AN3CA and HEC50B cells. The apoptotic effect of fludarabine was measured using the annexin-V/7-AAD apoptosis assay kit. (c) Caspase-3 protein induction by fludarabine. After 24-hr exposure to fludarabine, luminescence was gradually elevated in HEC1A cells in a dose-dependent manner, reflecting the activity of caspase-3/7, and this induction was almost sixfold higher than that in HEC50B cells ( $p < 0.001$ ). (d) Fludarabine efficacy *in vivo*. Mice inoculated with  $5 \times 10^6$  endometrial cancer cells subcutaneously were treated with fludarabine (125 mg/kg), sterile distilled water or cisplatin (1 mg/kg/day). Tumor growth was completely inhibited by cisplatin for mice inoculated with AN3CA ( $p < 0.05$ ). Tumor growth in HEC1A-inoculated mice was significantly inhibited by fludarabine ( $p < 0.05$ ). [Color figure can be viewed in the online issue, which is available at [wileyonlinelibrary.com](http://wileyonlinelibrary.com).]

100  $\mu$ M fludarabine (Fig. 3b). Conversely, no induction of apoptosis was observed in the HEC50B cells.

#### Fludarabine-induced caspase-3 activity

Caspase-3 activation is involved in cell death signaling and induces chromatin condensation and DNA fragmentation, resulting in apoptosis. Caspase-3 $\alpha$  and caspase-3 $\beta$  mRNA expression in HEC1A and AN3CA cells were upregulated by fludarabine in a dose-dependent manner ( $p < 0.05$ , Supporting Information Fig. 2A). HEC1A cells were still responsive to fludarabine at the lowest dose, 25  $\mu$ M, whereas a similar low-dose response was not evident in AN3CA cells. There was no change in expression levels of these genes in the HEC50B cells, even at 100  $\mu$ M. Similarly, caspase-3 protein expression increased in HEC1A cells after fludarabine treatment in a dose-dependent manner accompanied by a concomitant increase of cleaved-caspase-3 (Supporting Information Fig. 2B). Next, caspase-3/7 activity was assessed using a luminometer to investigate whether the upregulation

of caspase-3 expression in fludarabine-treated cells was related to the activity of caspase-3 in facilitating and inducing apoptosis. After 24-hr exposure to fludarabine, the luminescence was gradually elevated in HEC1A cells in a dose-dependent manner to reflect the activity of caspase-3/7, and this induction was almost sixfold higher than that observed in HEC50B cells ( $p < 0.001$ , Fig. 3c). The AN3CA cells also showed increasing luminescence but the slope of the increase was lower than that in HEC1A cells.

#### Therapeutic effects of fludarabine in a mouse xenograft model of endometrial cancer

We investigated the *in vivo* therapeutic effects of fludarabine, cisplatin and sterile water on subcutaneously inoculated HEC1A, AN3CA and HEC50B xenografts in CD-1 Foxn/Nu mice. Tumor growth was completely inhibited by cisplatin in mice inoculated with AN3CA cells, consistent with the high probability of cisplatin sensitivity predicted from the microarray analysis ( $p < 0.05$ , Fig. 3d). Growth-inhibitory effects of

fludarabine were not evident in AN3CA-inoculated mice, and there was no therapeutic effect of cisplatin or fludarabine on tumor growth of HEC50B-inoculated mice. On the other hand and also consistent with the predicted sensitivity, tumor growth in HEC1A-inoculated mice was indeed significantly inhibited by fludarabine ( $p < 0.05$ , Fig. 3*d*).

## Discussion

Endometrial carcinoma is frequently diagnosed at an early stage, at which point it is usually surgically curable. Surgical treatment includes hysterectomy, bilateral salpingo-oophorectomy and staging lymphadenectomy, which is a controversial but still common procedure in treating endometrial cancers. Adjuvant therapies to prevent relapse are mainly composed of platinum and doxorubicin or taxane, and are used for the patients bearing tumors with aggressive features such as pathologically high grade, invasion into the outer myometrium, lymphovascular space or cervix and extrauterine spread.<sup>13,14</sup> As shown in Table 2, the tumor recurrence rate in the group of intermediate-risk patients was significantly diminished by adjuvant chemotherapies, whereas recurrence was not improved in the high-risk group receiving similar therapies. Several randomized trials have reported effectiveness of adjuvant therapies. The carboplatin–paclitaxel regimen was previously reported as a well-tolerated and active regimen that provides a median time to progression of 13 months and a median overall survival of 47 months in high-risk patients.<sup>15</sup> The GOG 177 trial showed that addition of paclitaxel to the doxorubicin–cisplatin regimen significantly improved the rate of objective response and overall survival of high-risk or recurrent cases.<sup>5</sup> However, these results, such as the 57% of response rate and 17.3 months of overall survival, are not satisfactory in terms of therapeutic effect, and so the need for improved treatment strategies is urgently required to improve therapeutic benefit for patients with high-risk or recurrent disease.

The majority of high-risk or chemorefractory endometrial cancer cases are high grade, and the major challenge in developing more effective therapeutic strategies for these women involves confronting the heterogeneity of the disease and the distinct underlying mechanisms. The NCI60 database is comprised of more than 60 established cell lines from a diverse collection of malignant human tissues that have been tested for sensitivity to over 40,000 compounds to identify those with anticancer activity. Because of this diversity, the NCI60 is regarded as a reasonable representation of tumor heterogeneity and has been extensively used for discovering potent anticancer drugs.<sup>11,16,17</sup> Endometrial cancers are heterogeneous tumors that are classified into several types based on histological differentiation, and etiologic heterogeneity exists as well, especially within endometrioid adenocarcinoma. Thus, efforts have been made to establish molecular-based classifications, which may help in understanding the differences in biology and clinical outcome among subtypes.<sup>18</sup> In our study, 39% of the NCI60 cell lines were refractory to

cisplatin, doxorubicin or paclitaxel, and intriguingly, this rate is quite similar to the 44% of high-risk patients who are chemorefractory from our data. With the aim of prompt clinical translation, the GI50 values from the NCI60 data were analyzed for 24 agents already in clinical use, and the results indicated that none was promising for the high-risk patient population. However, as the anticancer drugs and the molecular-targeting drugs exhibit distinct spectra, combined therapy using agents from each group may be a reasonable and more effective approach for use as second-line chemotherapy.

Gene expression profiling studies have been valuable tools for revealing the complex nature of cancer and for identifying new therapeutic strategies.<sup>11</sup> As the NCI60 dataset includes gene expression information, a pharmacogenomics approach allows the ability to define common genetic backgrounds as “signatures” of chemorefractory cell lines and to identify candidate drugs potentially effective against these cell lines. Using Bayesian binary regression methods, a sensitivity gene expression signature for each candidate drug, based on the results of the NCI60 analysis, can be projected onto independent microarray datasets including those from endometrial cancers to predict the probability of drug sensitivity for each sample. As expected, the sensitivity probabilities of three conventional chemotherapeutic agents were low in high-grade endometrial cancers (Fig. 2*a*). In contrast, temsirolimus was predicted as a potentially effective agent against serous adenocarcinoma. Temsirolimus is a molecular targeting agent that functions by inhibiting mTOR pathway signaling, a pathway impaired in endometrial cancers. This agent is now being studied under a GOG clinical trial to investigate efficacy for chemorefractory endometrial cancers. Considering our analysis, temsirolimus may be effective in a subset analysis for histology even when the results of primary endpoint analysis for the entire population might be negative. In endometrial cancers, loss of PTEN correlates with poor outcomes,<sup>18</sup> and cell lines with little or no PTEN are preferentially sensitive to temsirolimus as cell viability and Akt phosphorylation were regulated by temsirolimus in a dose-dependent manner.<sup>19</sup> There are no reports showing interaction between the mTOR pathway and p53 mutations in serous endometrial cancers, but upregulation of mTOR is observed in invasive bladder cancer accompanied by deletion or mutation of p53,<sup>20</sup> which suggests that temsirolimus, as an mTOR inhibitor, might be useful in serous endometrial cancers in which p53 is frequently mutated.

By analyzing the complexity of the genomic signatures from the cell lines, fludarabine was also predicted as a potential candidate for chemorefractory high-grade cases. Among seven endometrial cancer cell lines that were resistant to cisplatin, doxorubicin and paclitaxel, five exhibited favorable probability of sensitivity to fludarabine, whereas only three of those seven exhibited a favorable probability score of sensitivity to temsirolimus (Supporting Information Table 2). These results suggest that fludarabine is a promising alternative agent for chemorefractory endometrial cancers.

The classes of antineoplastic drugs belonging to the group of purine nucleoside analogs play an important role and have had a substantial impact on the treatment of cancer.<sup>21–23</sup> Fludarabine is a purine analog that has demonstrated significant activity in B-cell malignancies, including CLL and indolent non-Hodgkin's lymphoma. Fludarabine is converted intracellularly into its active metabolite F-ara-ATP, which inhibits DNA as well as RNA synthesis, resulting in induction of growth arrest and apoptosis.<sup>24</sup> A single case report in the 1980s failed to show efficacy for recurrent endometrial cancers,<sup>25</sup> but as the number of cases was small and tumor histology was varied, it is hard to determine efficacy in high-grade tumors from this report. Our preliminary analysis for gene expression implies "purine metabolism" is augmented in G3 and serous endometrial cancers compared to G1 and G2 (data not shown), which is supportive of our prediction on fludarabine efficacy toward G3 and serous cases.

The exact mechanism of apoptosis induction by F-ara-A in proliferative and quiescent cells has not been completely clarified although purine nucleoside analogs are reported to activate d-ATP-dependent caspase pathways.<sup>26</sup> To investigate the cytotoxic effect of fludarabine, *in vitro* proliferation assays were done on three endometrial cancer cell lines, which were chosen as representative cell lines according to their probability of sensitivity to conventional chemo agents, as described in the Material and Methods section. As shown in Figure 3, fludarabine has a cytotoxic effect on endometrial cancer, inhibiting tumor growth and inducing apoptosis in a dose-dependent manner *in vitro*, suggesting that fludarabine may inhibit the proliferation of endometrial cancer cells

through induction of apoptosis, consistent with reports using Jurkat cells.<sup>24</sup> Caspase-3 is activated *via* death receptor signaling to induce chromatin condensation and DNA fragmentation, resulting in apoptosis.<sup>27,28</sup> In both HEC1A cells and AN3CA cells, caspase-3 was activated *in vitro* by fludarabine more than fivefold higher than in the HEC50B cells that are resistant to fludarabine. On the other hand, fludarabine was not inhibitory to tumor growth in AN3CA-inoculated mice, but robustly inhibited HEC1A-derived tumors. The reason for this difference is not clear, but as growth inhibition and induction of apoptosis *in vitro* were higher in HEC1A cells at a lower dose, it may be that drug delivery to the tumor tissue *in vivo* was not as effective. Furthermore, *Caspase-3* expression was increased, suggesting the possibility that this augmentation may play a role in determining susceptibility to fludarabine despite the belief that constitutive expression of caspase-3 is not usually considered significant in apoptosis. These results may imply the existence of an unknown mechanism(s) enhancing the efficacy of fludarabine in each tumor.

In our study, we have used a pharmacogenomics approach with drug-specific signatures as a targeted method to identify new candidate drugs with potential efficacy against chemoresistant endometrial cancers. Through array-based analysis, fludarabine and temsirolimus were identified as candidate chemotherapeutic agents for chemorefractory endometrial cancers. This prediction was confirmed both *in vitro* and *in vivo*. Although further study is warranted, fludarabine may prove beneficial as an addition to the treatment strategy for managing high-risk endometrial cancers.

## References

- Sorosky JL. Endometrial cancer. *Obstet Gynecol* 2008;111:436–47.
- Dizon DS. Treatment options for advanced endometrial carcinoma. *Gynecol Oncol* 2010;117:373–81.
- Huh WK, Powell M, Leath CA, III, et al. Uterine papillary serous carcinoma: comparisons of outcomes in surgical Stage I patients with and without adjuvant therapy. *Gynecol Oncol* 2003;91:470–5.
- Dizon DS, McCourt CK, Hanley TM, et al. Adjuvant therapy for endometrial cancer: "Sandwich therapy" of carboplatin and paclitaxel with radiation therapy. The Women and Infants' Hospital experience and review of the literature. *Cancer Ther* 2007;5:395–400.
- Fleming GF, Brunetto VL, Cella D, et al. Phase III trial of doxorubicin plus cisplatin with or without paclitaxel plus filgrastim in advanced endometrial carcinoma: a Gynecologic Oncology Group Study. *J Clin Oncol* 2004;22:2159–66.
- Symmans WF, Hatzis C, Sotiropoulos C, et al. Genomic index of sensitivity to endocrine therapy for breast cancer. *J Clin Oncol* 2010;28:4111–19.
- Kim SK, Yun SJ, Kim J, et al. Identification of gene expression signature modulated by nicotinamide in a mouse bladder cancer model. *PLoS One* 2011;6:e26131.
- Kwon JS, Mazgani M, Miller DM, et al. The significance of surgical staging in intermediate-risk endometrial cancer. *Gynecol Oncol* 2011;122:50–4.
- Kang HS, Baba T, Mandai M, et al. GPR54 is a target for suppression of metastasis in endometrial cancer. *Mol Cancer Ther* 2011;10:580–90.
- Bild AH, Parker JS, Gustafson AM, et al. An integration of complementary strategies for gene-expression analysis to reveal novel therapeutic opportunities for breast cancer. *Breast Cancer Res* 2009;11:R55.
- Matsumura N, Huang Z, Baba T, et al. Yin yang 1 modulates taxane response in epithelial ovarian cancer. *Mol Cancer Res* 2009;7:210–20.
- Mori S, Chang JT, Andrechek ER, et al. Anchorage-independent cell growth signature identifies tumors with metastatic potential. *Oncogene* 2009;28:2796–805.
- Hsiao SM, Wei LH. Controversies in the adjuvant therapy of endometrial cancer. *ISRN Obstet Gynecol* 2011;2011:724649.
- Ray M, Fleming G. Management of advanced-stage and recurrent endometrial cancer. *Semin Oncol* 2009;36:145–54.
- Sovak MA, Hensley ML, Dupont J, et al. Paclitaxel and carboplatin in the adjuvant treatment of patients with high-risk stage III and IV endometrial cancer: a retrospective study. *Gynecol Oncol* 2006;103:451–7.
- Holbeck SL, Collins JM, Doroshow JH. Analysis of Food and Drug Administration-approved anticancer agents in the NCI60 panel of human tumor cell lines. *Mol Cancer Ther* 2010;9:1451–60.
- Kondoh E, Mori S, Yamaguchi K, et al. Targeting slow-proliferating ovarian cancer cells. *Int J Cancer* 2010;126:2448–56.
- Yang HP, Wentzensen N, Trabert B, et al. Endometrial cancer risk factors by 2 main histologic subtypes: the NIH-AARP Diet and Health Study. *Am J Epidemiol* 2013;177:142–51.
- Yang S, Xiao X, Meng X, et al. A mechanism for synergy with combined mTOR and PI3 kinase inhibitors. *PLoS One* 2011;6:e26343.
- Puzio-Kuter AM, Castillo-Martin M, Kinkade CW, et al. Inactivation of p53 and Pten promotes invasive bladder cancer. *Genes Dev* 2009;23:675–80.
- Robak T, Korycka A, Kasznicki M, et al. Purine nucleoside analogues for the treatment of hematological malignancies: pharmacology and clinical applications. *Curr Cancer Drug Targets* 2005;5:421–44.
- Robak T, Korycka A, Lech-Maranda E, et al. Current status of older and new purine

- nucleoside analogues in the treatment of lymphoproliferative diseases. *Molecules* 2009;14:1183–226.
23. Zhenchuk A, Lotfi K, Juliusson G, et al. Mechanisms of anti-cancer action and pharmacology of clofarabine. *Biochem Pharmacol* 2009;78:1351–9.
24. Nishioka C, Ikezoe T, Togitani K, et al. Fludarabine induces growth arrest and apoptosis of cytokine- or alloantigen-stimulated peripheral blood mononuclear cells, and decreases production of Th1 cytokines via inhibition of nuclear factor kappaB. *Bone Marrow Transplant* 2008;41:303–9.
25. Von Hoff DD, Green S, Alberts DS, et al. Phase II study of fludarabine phosphate (NSC-312887) in patients with advanced endometrial cancer. A Southwest Oncology Group Study. *Am J Clin Oncol* 1991;14:193–4.
26. Faria JR, Yamamoto M, Faria RM, et al. Fludarabine induces apoptosis in chronic lymphocytic leukemia—the role of P53, Bcl-2, Bax, Mcl-1, and Bag-1 proteins. *Braz J Med Biol Res* 2006;39:327–33.
27. Porter AG, Janicke RU. Emerging roles of caspase-3 in apoptosis. *Cell Death Differ* 1999;6:99–104.
28. Baran Y, Oztekin C, Bassoy EY. Combination of fludarabine and imatinib induces apoptosis synergistically through loss of mitochondrial membrane potential and increases in caspase-3 enzyme activity in human K562 chronic myeloid leukemia cells. *Cancer Invest* 2010;28:623–8.